LAWRENCE
LIVERMORE
NATIONAL
LABORATORY

LLNL-JRNL-447554

Predicting laser-induced bulk damage and conditioning for deuterated potassium di-hydrogen phosphate crystals using ADM (absorption distribution model)

Z. M. Liao, M. L. Spaeth, K. Manes, J. J. Adams, C. W. Carr

August 5, 2010

Optics Letters

Disclaimer

Predicting laser-induced bulk damage and conditioning for deuterated potassium di-hydrogen phosphate crystals using ADM (absorption distribution model)

Z. M. Liao, M. L. Spaeth, K. Manes, J. J. Adams, and C. W. Carr

Lawrence Livermore National Laboratory, 7000 East Ave., Livermore, CA 94550

We present an empirical model that describes the experimentally observed laser-induced bulk damage and conditioning behavior in deuterated Potassium dihydrogen Phosphate (DKDP) crystals in a self-consistent way. The model expands on an existing nano-absorber precursor model and the multi-step absorption mechanism to include two populations of absorbing defects, one with linear absorption and another with nonlinear absorption. We show that this model connects previously uncorrelated small-beam damage initiation probability data to large-beam damage density measurements over a range of ns pulse widths relevant to ICF lasers such as the National Ignition Facility (NIF). In addition, this work predicts the damage behavior of laser-conditioned DKDP and explains the upper limit to the laser conditioning effect. The ADM model has been successfully used during the commissioning and early operation of the NIF.

Potassium dihydrogen phosphate (KDP) and it's deuterated analog (DKDP) crystals are important materials on large aperture laser systems such as the National Ignition Facility (NIF) and the Laser Megajoule (LMJ)[1] because of the large (~700 lbs) sizes which single crystals can be grown. Plates of these crystals are typically used for nonlinear conversion processes and for polarization rotation. The NIF uses KDP for Second Harmonic Generation (SHG) of 527 nm light and DKDP for sum frequency mixing, i.e. 1053 nm + 527 nm = 351 nm or Third Harmonic Generation (THG). As shorter wavelengths typically have a greater propensity to produce damage[2], these crystals are subject to damage from the converted light they generate[3]. In addition to the large sizes to which these crystals can be grown, another useful aspect of these crystals is that they exhibit laser conditioning[4], i.e. the laser damage threshold of the material increases after exposure to sub-damaging laser fluences. Over the last two decades, there has been numerous studies focusing on the damage behavior of these crystals[3, 5-12]. Some of these experiments probed the damage probability as a function of fluence using small (~1 mm^2) beam damage tests, i.e. single-fluence-multiple-shot tests (S/1) or ramped-fluence-single-shot tests (R/1)[13], while others measured damage density ($\rho(\phi)$) directly[14]. Furthermore, laser parameters such as pulse width[1] and pulse shape dependence[15] have been studied and attempts have been made to explain specific aspects of the observed behavior[2, 16, 17] but a universal description has remained elusive. In this work we propose an empirical model that that can self-consistently explain a large set of diverse data such as the connection between parallel measurement types of damage density and damage probability (i.e. S/1 vs. R/1 vs. $\rho(\phi)$) as well as providing accurate predictions for conditioning of KDP and DKDP crystals.

Feit and Rubenchik have developed a physical model describing laser-induced damage of linearly absorptive homogenous precursors in the bulk of a material based on a general thermal diffusion model. Their model assumes that damage occurs when precursors absorb sufficient laser energy to reach some critical temperature. In 2003, Carr observed sharp drops in the damage threshold at photon energies corresponding to integer fractions of the KDP band gap[2]. He proposed that the damage precursors were defect clusters which absorbed light with a multi-step absorption mechanism. Our work[18] builds on these previous models and adds another dimension; the precursor defects are not homogenously composed but are made up of (at least) two distinct populations of defect clusters, one of which absorbs linearly and the other nonlinearly. Furthermore, as a given size precursor can be composed of various densities of the

individual defect types (i.e. absorption values), there should be a distribution in absorption for any given precursor size (see Figure 1).

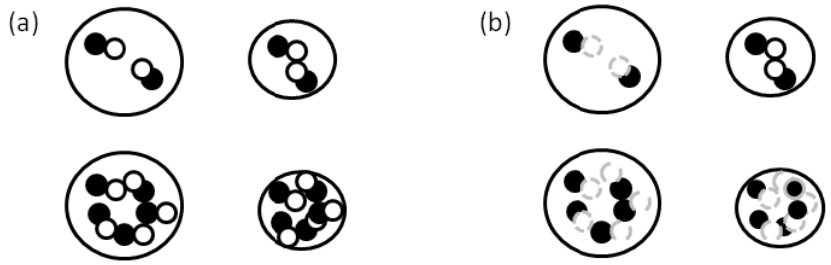

Figure 1: Precursors of different size and density of defects (i.e. absorption) for unconditioned part (a) and partially conditioned part (b). Linearly absorbing defects (Type 1) are drawn as black balls while nonlinear absorbing defects (Type 2) are drawn as black circles. Conditioned Type 2 defects are drawn as gray circles.

The Absorption Distribution Model (ADM) starts with the thermal diffusion equation[19] that describes a spherical precursor embedded in a bath of room temperature bulk material

$$\frac{\partial \Theta}{\partial t} = \frac{\alpha(I) I}{\rho C_p} + \nabla \cdot (D \nabla \Theta), \tag{1}$$

where Θ is the relative temperature rise at the center of the precursor, I is the intensity of the laser, α is the (intensity dependent) absorption, ρ is the mass density, C_p is the specific heat, and D is the thermal diffusivity of the material[20]. The time-dependent temperature Θ(t) can be solved using the Green's function. Whereas the Feit-Rubenchik model would predict an absorption dominated only by the precursor size, a (α ∝ a), ADM requires both a distribution in precursor size and a distribution in absorption that comes from variations of defect densities in precursors as follows

$$N(a,\alpha) = n(a) f(\alpha) \tag{2}$$

Here n(a) is the number density of precursor size, a, and f(α) is the probability distribution function of defect cluster densities (i.e. precursor absorption), α. In addition, ADM also allows for intensity dependent nonlinear absorption α(I) which can be expanded in a power series as

$$\alpha(I) = \alpha_1 + \alpha_2 f(I) = \alpha_1 + \alpha_2 \left(c_0 + c_1 I + c_2 I^2 + c_3 I^3 + ... + c_n I^n \right) \tag{3}$$

where c_n's are the coefficients of different orders of intensity-dependent nonlinear absorption. We have found that a Gaussian distribution does a good job of describing a given precursor size's defect cluster population, which translates to an absorption distribution. Each defect type absorption distribution can be characterized by its mean (μ) and variance (σ) as follow

$$f(\alpha) = \frac{1}{\sqrt{2\pi}\sigma} e^{\frac{-(\alpha-\mu)^2}{2\sigma^2}} \tag{4}$$

If we assumed that the two absorption distributions, which we shall label Type 1 and Type 2, are completely correlated (i.e. highest absorption for Type 1 also corresponds to highest absorption for Type 2), then the total absorption distribution for a precursor size is just the sum of the individual distributions

$$\mu_T = \mu_1 + \mu_2 \qquad \sigma_T = \sigma_1 + \sigma_2 \tag{5}$$

The critical parameter that governs damage initiation is the maximum temperature rise in time (Θ_m) and damage initiation occurs whenever local temperature exceeds a critical damage initiation temperature, Θ_x, i.e. $\Theta_m > \Theta_x$ for that material at a given fluence and material absorption. We believe this critical temperature is an intermediate temperature that causes the surrounding bulk of the material to change such that runaway absorption occurs, and damage ensues. The portion of a given precursor size that damages on a given shot (i.e. damage probability) can be calculated as follows

$$\mathrm{P}(\varphi, a) = \int_{\alpha_x(\varphi,a)}^{\infty} f(\alpha) \cdot d\alpha \tag{6}$$

where α_x is the threshold absorption for a given precursor size, a, to achieve Θ_x at fluence ϕ.

Laser conditioning occurs when the local temperature reaches a critical conditioning temperature, Θ_c, causing Type 2 precursors to be less absorbing as follow

$$\alpha_2 \rightarrow \alpha_2{}^* = C_f \cdot \alpha_2 \tag{7}$$

where C_f is the conditioning coefficient ($\leq$ 1). This conditioning process can be thought of as either uniformly reducing the absorption behavior of the Type 2 defect clusters or "destroying" a proportion of

the Type 2 defect clusters. The density of damage sites as a function of fluence can be computed by integrating over the precursor size distribution as follows

$$\rho(\phi) = \int_{a_{\min}}^{a_{\max}} n(a)\mathrm{P}(\phi)da \tag{8}$$

We found that n(a) can be approximated with power law dependence ($\propto a^b$) by comparing this formulation to experimental measurements. The minimum a_{min} and maximum, a_{max} precursor sizes of 50 nm and 500 nm respectively are consistent with the observed sizes of damage sites[21] and with the smallest size suitable for absorbing energy in sufficient density[17].

Small aperture 3ω damage testing on a discrete number of sites using ~1 mm^2 test beams has been used to obtain a probability of damage on a single shot (S/1) or multiple shots of increasing fluence (R/1). R/1 is a measurement of maximal conditioning effects – as the R/1 damage threshold is still substantially smaller than the material damage threshold. In terms of ADM theory, the S/1 and R/1 results delineate clearly the unconditioned (S/1) and "best conditioned" (R/1) scenarios, as a result, S/1 and R/1 can also be used to extract the absorption parameters for population Types 1 and 2. S/1 and R/1 data is often collected for the larger crystals produced for NIF. Damage density, $\rho(\phi)$, data is generally less available and has not been measured for all of NIF's crystals. Using Eq. 6 which returns $P(\phi)$ given the population distribution for α, we can extract the Type 1 defect population parameters using R/1 data (see Figure 2) since the Type 2 population is assumed to be completely conditioned during the fluence ramp (i.e. $C_f = 0$ or $\alpha = \alpha_1$). The S/1 data can then be analyzed (using Eq. 6) to obtain Type 2 defect population parameters since both populations are present (i.e. $\alpha = \alpha_1 + \alpha_2 f(I)$) with α_1 having already been derived from R/1 data. When a sample has been exposed to a large beam laser, it should be partially conditioned with the conditioning coefficient accounting for effectiveness of conditioning. The S/1 data for partially conditioned DKDP (S/1C) is shifted to the right of unconditioned S/1 data (see Figure 2) and the conditioning coefficient C_f can be derived from this data. However, R/1 data that has been partially conditioned (R/1C) differs little from unconditioned R/1 data.

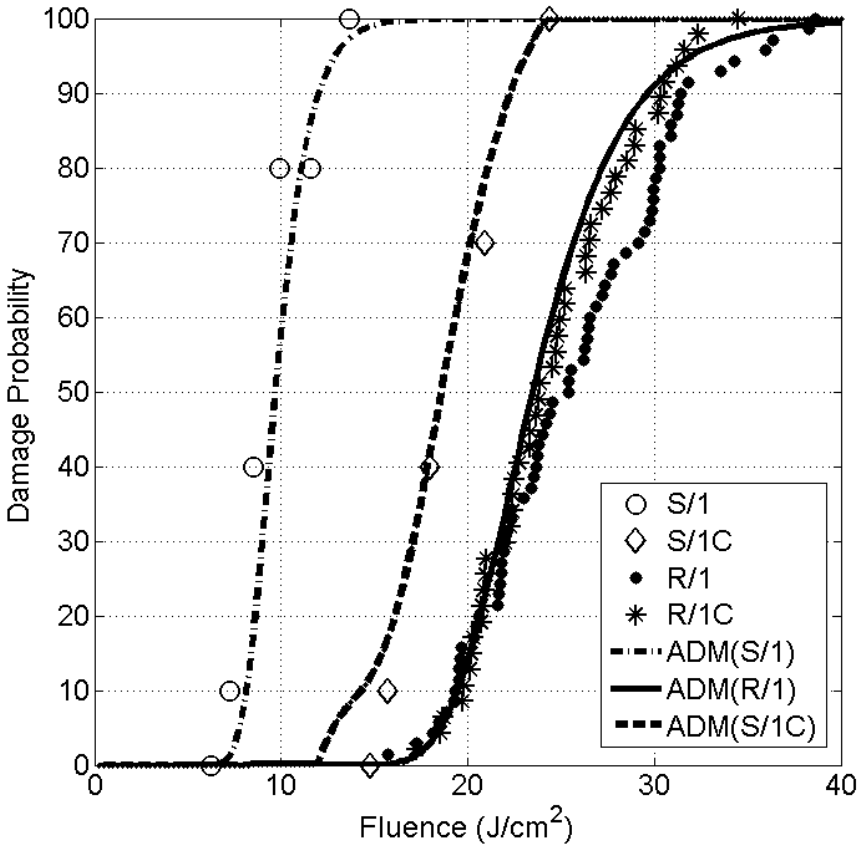

Figure 2. Measured 3ω S/1 and R/1 test results for an unconditioned and conditioned (at 8 J/cm^2 with 3.4ns Gaussian pulse shape) DKDP crystal (boule LL16), along with ADM predictions using the absorption population values extracted from the data. A conditioning coefficient of C_f=0.15 is used in the calculation.

Once the defect population are known, the damage density, $\rho(\phi)$ can be computed using Equation 8 given a precursor size distribution n(a). In Figure 3, we show the unconditioned and conditioned $\rho(\phi)$ damage test results from the same crystal that provided the S/1 and R/1 data[14]. The conditioning was achieved by pre-exposing the part to 10 J/cm^2 with 3.5 ns Gaussian pulse at 3ω. The ADM predictions for both the unconditioned and conditioned $\rho(\phi)$ use the same defect population as well as precursor size distribution (a_{min}=50 nm, a_{max}=500 nm, b = 3) and agree remarkably well with the experimental data.

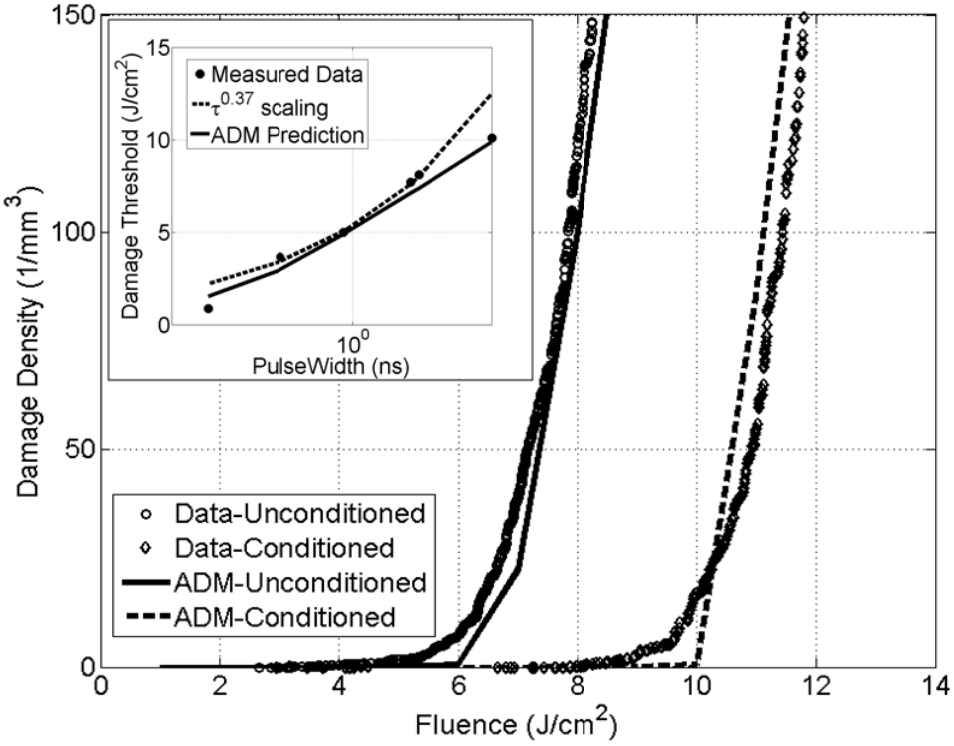

Figure 3. Measured and ADM-predicted 3ω, 3.5ns Gaussian pulse ρ(ϕ) for unconditioned and conditioned DKDP crystal (boule LL16). Conditioning was performed at 10 J/cm^2 with a 2.85 ns Gaussian pulse. Insert: Measured and ADM-predicted 3ω damage threshold ϕ_{th} vs. Gaussian pulsewidth for DKDP crystal (boule LL16).

Damage initiation dependence on pulse length has been elusive because of difficulties obtaining good data that span the relevant pulsewidths. Recent data consist of measurements of the light scattered by sites initiated on crystal LL-16 using damaging pulses of different Gaussian pulsewidth. The scatter data were recast as $\rho(\phi, \tau)$ data by using the measured damage site size as a function of pulse duration[22]. Each of the constructed $\rho(\phi, \tau)$ provides a threshold data point $\phi_{th}(\tau)$ which is defined as the fluence at that pulsewidth that yield $\rho(\phi_{th}, \tau) \sim 20$ pinpoints/mm^3 (see Figure 3 insert). The ADM prediction follows the threshold data quite closely, which is remarkable since the parameters used in the model, i.e. defect population as well as precursor size distribution, were extracted using a separate set of damage data (i.e. S/1, R/1, etc.). From this boule, the coefficients that best represent the data were c_0=1, c_1=0.15, and

c_2=0.05. It is clear that the damage threshold is not adequately described by a simple power-law scaling ($\tau^{0.37}$), but ADM was able to capture this complexity.

ADM can also reproduce the effect of pulse shape on the damage behavior of DKDP crystals, which has been observed experimentally. Figure 4 show a set of 3ω damage ρ(ϕ) data obtained from samples of boule LL32 with a 2.9-ns Gaussian pulse shape as well as a 2.85 ns flat-in-time (FIT) pulse shape. The associated ADM predictions use Type 1 and Type 2 absorption population parameters extracted from analysis of S/1 and R/1 test data for this same boule. The predictions use the same precursor size distribution, the only difference in the calculation being the pulse shape (i.e. the intensity, I(t) of the laser used in Eq. 1). ADM was able to successfully predict the pulse shape dependence of damage density. Small discrepancies in the ADM prediction for the Gaussian pulse shape can be attributed to the fact that the calculation uses ideal Gaussian pulses as input rather than the measured pulse shapes.

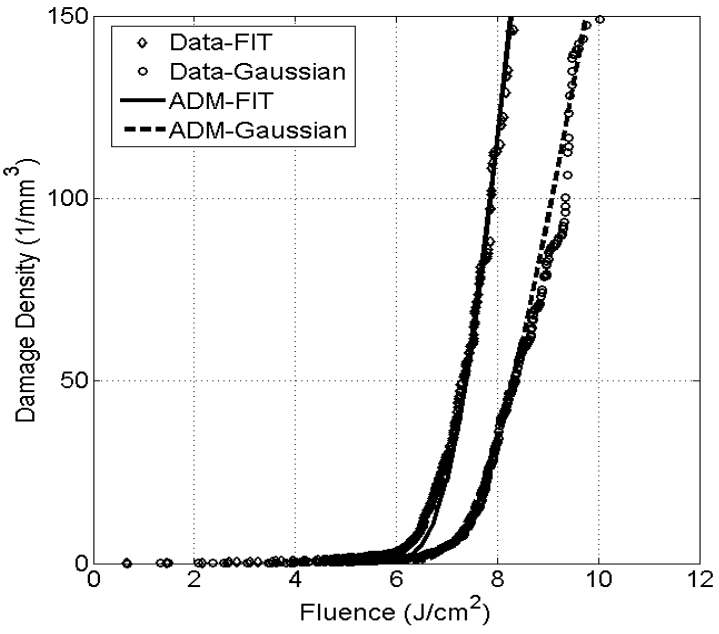

Figure 4: Measured and ADM-predicted 3ω ρ(ϕ) for Gaussian and FIT pulses for DKDP crystal from boule LL32.

In conclusion, we present ADM as a model for calculating the damage density of unconditioned as well conditioned DKDP crystals using threshold probability measurements. This new model integrates successful aspects of past models and allows accurate predictions of the effect of pulse duration as well as pulse shape on damage initiation and conditioning. Although ADM does not uniquely identify defect clusters sizes or their locations in the crystal, this information is not needed to make accurate predictions for damage initiation and optimal conditioning[23]. The ability of this model to simultaneously explain the different experimental results makes it an effective tool in predicting the damage behavior of DKDP crystals by leveraging already existing or easier to obtain data such as S/1 and R/1 threshold measurements or damage density measurements at a specific pulse shape and pulse length.

Acknowledgements

The authors would like to thank Dr. Paul J. Wegner for his helpful review of this manuscript and the OSL crew for their dedication and high standards. This work is performed under the auspices of the U.S. Department of Energy by Lawrence Livermore National Laboratory under Contract DE-AC52-07NA27344 and funded through LLNL office of LDRD. (LLNL-NNN-xxxxxx).

References

[1] E. M. Campbell, Fusion Technology **26**, 755 (1994).
[2] C. W. Carr, *et al.*, Physical Review Letters **91**, 127402 (2003).
[3] C. W. Carr, *et al.*, Optics Letters **31**, 595 (2006).
[4] J. J. Adams, *et al.*,SPIE **5647**, 265 (2004).
[5] J. Swain, *et al.*, Applied Physics Letters **40**, 350 (1982).
[6] A. Yokotani, *et al.*, Applied Physics Letters **48**, 1030 (1986).
[7] M. Runkel, *et al.*,SPIE, 374 (1998).
[8] M. Staggs, *et al.*,SPIE **4347**, 400 (2000).
[9] H. Yoshida, *et al.*, Applied Physics B-Lasers and Optics **70**, 195 (2000).
[10] N. Balamurugan, *et al.*, Crystal Growth & Design **6**, 1642 (2006).
[11] R. A. Negres, *et al.*,SPIE **6720**, 72019 (2008).
[12] P. DeMange, *et al.*, Optics Letters **30**, 221 (2005).
[13] J. Adams, *et al.*,SPIE **6720** (2008).
[14] C. W. Carr, *et al.*, Measurement Science & Technology **17**, 1958 (2006).
[15] C. W. Carr, *et al.*, Applied Physics Letters **90** (2007).
[16] J. B. Trenholme, *et al.*,SPIE **5991** (2005).
[17] M. D. Feit, *et al.*,SPIE **5273**, 74 (2003).
[18] M. Spaeth, (LLNL Internal Presentation, 2007).
[19] M. D. Feit, *et al.*,SPIE **5273**, 74 (2004).
[20] R. W. Hopper, *et al.*, Journal of Applied Physics **41**, 4023 (1970).
[21] C. W. Carr, *et al.*, Applied Physics Letters **89** (2006).
[22] C. W. Carr, *et al.*,SPIE **6403** (2007).
[23] Z. M. Liao, *et al.*, in *OSA Nonlinear Optics Conference* (OSA, Honolulu, Hawaii, 2009).